

General Disclaimer

One or more of the Following Statements may affect this Document

- This document has been reproduced from the best copy furnished by the organizational source. It is being released in the interest of making available as much information as possible.
- This document may contain data, which exceeds the sheet parameters. It was furnished in this condition by the organizational source and is the best copy available.
- This document may contain tone-on-tone or color graphs, charts and/or pictures, which have been reproduced in black and white.
- This document is paginated as submitted by the original source.
- Portions of this document are not fully legible due to the historical nature of some of the material. However, it is the best reproduction available from the original submission.

Discrete Element Modeling (DEM) of Triboelectrically Charged Particles: Revised Experiments

M.D. Hogue
Electrostatics & Surface Physics Laboratory
NASA, Kennedy Space Center
KSC, FL USA 32899
phone: (1) 321-867-7549
e-mail: Michael.D.Hogue@nasa.gov

C.I. Calle
Electrostatics & Surface Physics Laboratory
NASA, Kennedy Space Center
KSC, FL USA 32899
e-mail: Carlos.I.Calle@nasa.gov

D.R. Curry
DEM Solutions, Inc.
20 York Place
Edinburgh, UK EH1 3EP
e-mail: dcurry@dem-solutions.com

P.S. Weitzman
DEM Solutions (USA) Inc.
24 Hanover Street, Suite 10
Lebanon, New Hampshire, 03766

Abstract— In a previous work, the addition of basic screened Coulombic electrostatic forces to an existing commercial discrete element modeling (DEM) software was reported. Triboelectric experiments were performed to charge glass spheres rolling on inclined planes of various materials. Charge generation constants and the Q/m ratios for the test materials were calculated from the experimental data and compared to the simulation output of the DEM software. In this paper, we will discuss new values of the charge generation constants calculated from improved experimental procedures and data. Also, planned work to include dielectrophoretic, Van der Waals forces, and advanced mechanical forces into the software will be discussed.

I. INTRODUCTION

Theoretical and experimental work was presented on the incorporation of screened Coulombic electrostatic force into a discrete element modeling (DEM) software used to model particle flow [1]. Experimental values of a triboelectric charging constant, α , was used to calculate simulated values of Q/m for comparison to experimental values of Q/m . The experimental procedure was changed to insure better discharging of the glass spheres used prior to the start of each experiment. The resulting values of α give values of Q/m in the DEM simulation that compare better to experimental ones.

Work is proceeding on incorporating advanced electrostatic forces into the DEM software such as the dielectrophoretic and Van der Waals forces. This work is part of a larger project with Glenn Research Center (GRC) and DEM Solutions, Inc. to expand the capability of the current EDEM™ software for planetary as well as terrestrial applications. The Kennedy Space Center (KSC) is working on methods to mitigate dust on the Moon and Mars [2]. One of these methods uses applied AC electric fields to move the dipolar dust simulants off of surfaces. Accurate computer modeling of this electrostatic dust screen is a goal of this project.

II. REVISED EXPERIMENTS

A. Procedure Modifications

The experiment consists of an inclined plane apparatus to triboelectrify 2.0 mm diameter borosilicate glass spheres that roll down the plane [1]. In the previous experiments, the means of neutralizing any initial charge on the spheres was inefficient due to the fact that spheres interior to the pile inside the sphere cup were shielded from the deionizer by the outer spheres. This resulted in simulation values of Q/m that did not match experimental values well [1]. This apparatus is shown in Fig. 1.

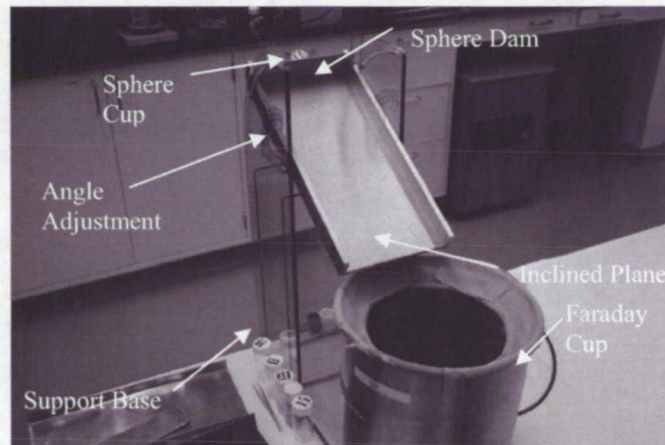


Fig. 1. Triboelectric apparatus with aluminum inclined plane, sphere cup, and dam. Total charge of the glass spheres, Q , is measured in the Faraday cup shown.

To reduce the initial triboelectric charge on the glass spheres, the experimental procedures were modified to allow better deionization of the spheres prior to each experiment. 25 spheres were used instead of 500 as before. This number of spheres was easier to deionize in the sphere cup prior to the experiment while still providing sufficient spheres to observe the flow pattern on the inclined plane.

The inclined plane was set at 30°. The inclined plane materials used were Aluminum, polyvinyl chloride (PVC), low density polyethylene (LDPE), Nylon 6/6, and polytetrafluoroethylene (PTFE). To remove any initial electrostatic charge, the spheres are discharged by use of an air ionizer. The spheres are then allowed to roll down the inclined plane into the Faraday cup by removing the sphere dam. The time of triboelectric contact with the inclined plane was measured by a stop watch. The sphere cup, dam, and inclined plane are all of the same material to insure that the triboelectric charging is caused by contact only against the test material.

B. Data

Ten experiments were performed for each inclined plane material and the results averaged. The values of Q/m and α from these experiments are summarized in Table 1.

TABLE 1: VALUES OF Q/m AND α FOR REVISED 30° EXPERIMENTS (RANGES ARE \pm ONE STANDARD DEVIATION)

Inclined Plane Material	Q/m (nC·g ⁻¹)	α (s ⁻¹)
Aluminum	0.524 \pm 0.363	0.023 \pm 0.015
PVC	5.874 \pm 1.610	0.237 \pm 0.042
LDPE	0.524 \pm 0.187	0.018 \pm 0.005
Nylon 6/6	1.459 \pm 0.411	0.057 \pm 0.012
PTFE	2.469 \pm 0.561	0.100 \pm 0.015

C. Data Analysis

Comparison of previous values of α [1] with the values in Table 1 are shown in Fig. 2. The much larger α values in Fig. 2 lead to better agreement between the EDEM simulation and experimental values of Q/m . This data is shown in Fig. 3. These revised experiments highlight the sensitivity of α to the initial conditions of the surfaces in question and the physical environment. More on this will be discussed in Sections III A and III B.

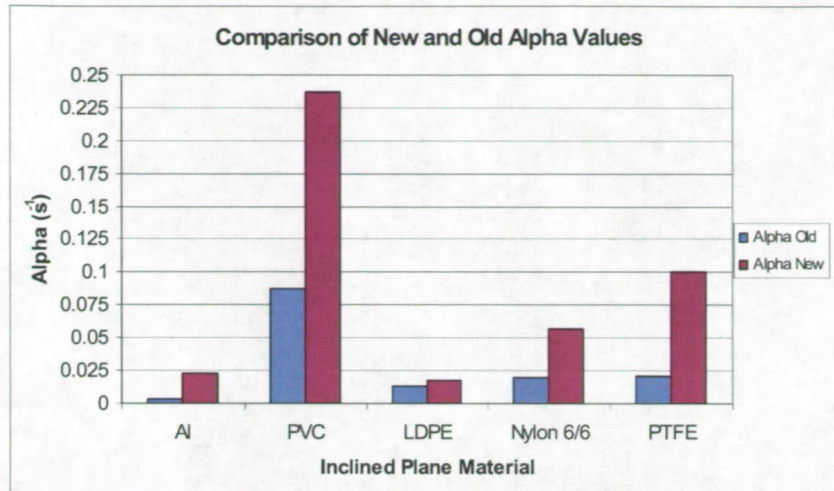


Fig. 2. Comparison of new and old values of the charge generation constant α .

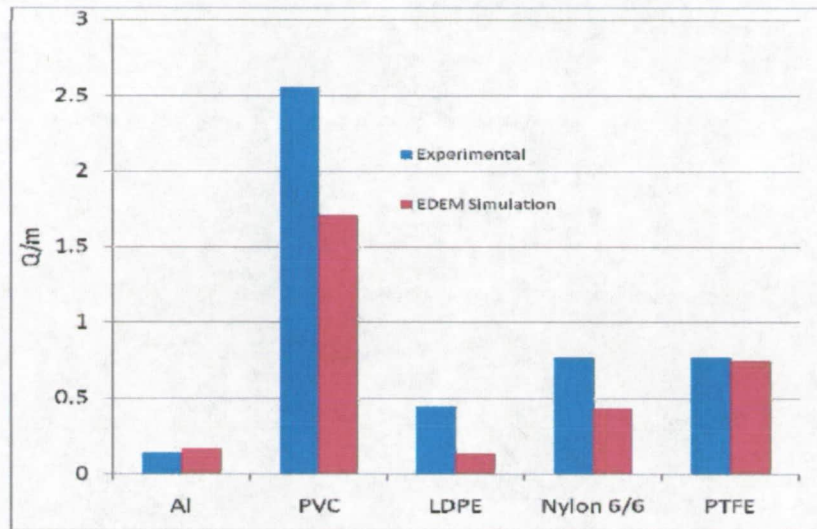


Fig. 3. Comparison of EDEM simulation and experimental values of Q/m using the new charge generation constant. Q/m values are given in $\text{nC}\cdot\text{g}^{-1}$.

III. THEORETICAL ASPECTS

A. Charge Dissipation Constant

The data analysis in section II highlights one of the inherent difficulties in using experimental values of the charge generation constant in that experimentally derived values of

the constant can be influenced by initial charge on the surfaces of the contacting bodies. This can be especially true when the model equation used assumes zero initial charge on the contacting surfaces[1][3] when there is some initial charge.

Potential parameters of α include, but are not necessarily limited to, temperature, pressure, % relative humidity, perpendicular force, parallel velocity, surface area, work function, and number of occupiable surface sites. The first three are environmental factors, the next two are kinematic factors, and the last three are material specific factors. The environmental factors can play significant roles in determining the value of α especially for insulators [4][5]. More on the initial charge will be discussed in section B.

B. Revised Triboelectric Charge Generation Equation

Many tribocharging situations of interest will have initial charge on the particles. To account for initial charge on the spheres, Greason's triboelectric charge generation equation [3],

$$\frac{dq}{dt} = \alpha(q_s - q) - \beta q, \quad (1)$$

is re-integrated but this time with limits on the charge integral of $q = q_0$ at $t = 0$ instead of $q = 0$ at $t = 0$. Here α and β are the charge generation and dissipation constants respectively and q_s is the saturation charge (here taken to be atmospheric breakdown). Performing this integration gives

$$q(t) = q_0 e^{-(\alpha+\beta)t} + \frac{q_s}{1 + \beta/\alpha} [1 - e^{-(\alpha+\beta)t}]. \quad (2)$$

The second term of Eq. (3) is the Greason equation discussed in [1] while the first term deals with initial charge on the spheres. Assuming negligible charge dissipation during the time frame of the inclined plane experiment ($\beta \approx 0$), we get

$$q(t) = q_0 e^{-\alpha t} + q_s (1 - e^{-\alpha t}). \quad (3)$$

For many particles, we multiply Eq. (3) through by the total number of particles, N , and rearrange to get

$$Nq(t) = Q(t) = Nq_s - (Nq_s - Q_0) e^{-\alpha t}. \quad (4)$$

Here, Q_0 is the total initial charge on all the particles. To use Eq. (4) one would have to measure the initial charge on the particles, Q_0 , before the start of any tribocharging experiment or process. For our inclined plane experiment, we would need to measure the total charge on the glass spheres in the sphere cup prior to removal of the dam. A way to do this is to replace the sphere cup with a second Faraday cup as the sphere reservoir. This will also allow Q/m measurements to be taken both before and after the triboelectric

charging. Eq. (4) can be solved for the triboelectric charging constant α .

$$\alpha = -\frac{1}{t} \ln \left[\frac{Nq_s - Q(t)}{Nq_s - Q_0} \right]. \quad (5)$$

Here the parameters N , $Q(t)$, Q_0 , and t are measured quantities while the saturation charge, q_s , for the inclined plane experiment is the electrical breakdown limit of air under standard conditions ($2.66 \times 10^{-5} \text{ C} \cdot \text{m}^{-2}$) [1].

C. Electrostatic Force Between a Particle and a Plane

Another factor to be considered is the electrostatic attraction between the spheres and the inclined plane (or other planar surfaces). Initial spheres from the sphere cup will encounter an uncharged plane (the plane was discharged prior to each experiment). However, the initial rolling spheres will tribocharge the plane and subsequent spheres will encounter an oppositely charged plane. The resulting attractive electrostatic force will have to be taken into account as a retarding force on the spheres like air resistance and friction.

The electrostatic attraction between a particle and a plane can be physically modeled by a charged particle of radius b above a charged circular surface area of radius a . To make a point charge approximation, let $b \ll a$ and the surface charge density on the circular area, σ , be uniform and constant. This is shown in Fig. 4.

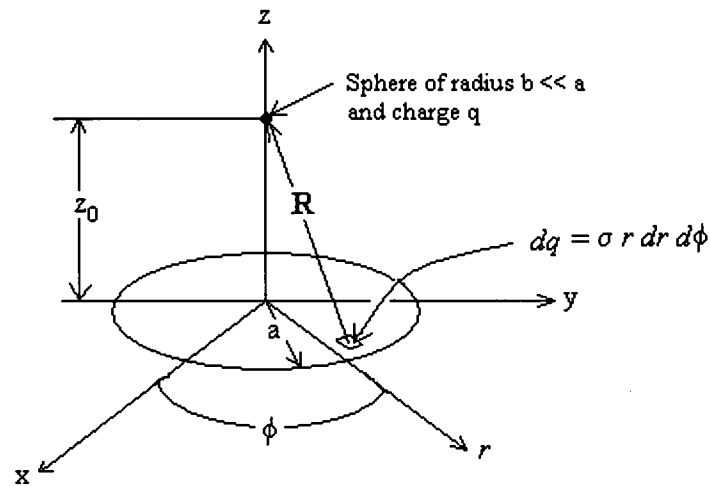


Figure 4. Charged particle of radius b near a charged circular plane of radius a .

In cylindrical coordinates, the unit vector \mathbf{R} is given by [6][7]

$$\vec{R} = -r\hat{r} + z_0\hat{z} \quad \text{with} \quad \frac{\vec{R}}{|\vec{R}|} = \frac{-r\hat{r} + z_0\hat{z}}{\sqrt{r^2 + z_0^2}}. \quad (6)$$

Using Eq. (6) and the geometry from Fig. 4, the differential force element can then be written as [6]

$$d\vec{F} = \frac{q}{4\pi\epsilon_0 R^2} \left(\frac{-r\hat{r} + z_0\hat{z}}{\sqrt{r^2 + z_0^2}} \right) \sigma r dr d\phi. \quad (7)$$

Before Eq. (7) is integrated, it should be noted that all the radial components will cancel from symmetry. Integrating Eq. (7) gives

$$\vec{F} = \frac{q\sigma}{4\pi\epsilon_0} \int_0^{2\pi} \int_0^a \frac{r}{(r^2 + z_0^2)^{3/2}} dr d\phi \hat{z} = \frac{q\sigma z_0}{2\epsilon_0} \left(\frac{1}{z_0} - \frac{1}{\sqrt{a^2 + z_0^2}} \right) \hat{z}. \quad (8)$$

Letting $z_0 \approx b$ for close proximity between the sphere and other surfaces we get

$$\vec{F} \cong \frac{q\sigma}{2\epsilon_0} \left(1 - \frac{b}{\sqrt{a^2 + b^2}} \right) \hat{z}. \quad (9)$$

Eq. (9) can be used to approximate the electrostatic force between a charged particle and a charged surface.

IV. DEM SIMULATION

DEM Solutions, Inc. has performed additional particle-particle and particle-surface triboelectric simulations modeling a physical situation similar to the experiment described in Section II. In this simulation [12], four angles (0° , 15° , 30° , 45°) are modeled simultaneously. This geometry is shown in Fig. 5. Box structures are used as the particle factories. The generic particles (20 for each factory) modeled are 0.5 mm in diameter with a mean density of $1200 \text{ kg} \cdot \text{m}^{-3}$ and a shear modulus of $7.7 \times 10^6 \text{ Pa}$. The charge generation constant, α , was set at -0.5 s^{-1} to insure that the particles would charge negatively and the sloped trough would charge positively.



Figure 5. EDEM Model of four inclined curved surfaces at 0°, 15°, 30°, and 45°. Box structures on the end are the particle factories.

Charge build-up on the inclined surfaces are calculated in EDEM and are shown graphically in Fig. 6. The higher charge build-up on the lower inclines is due to the longer contact time of the spheres. Additional normal force due to gravity in the lower inclines is negligible with such small particles but could be a factor for larger ones.

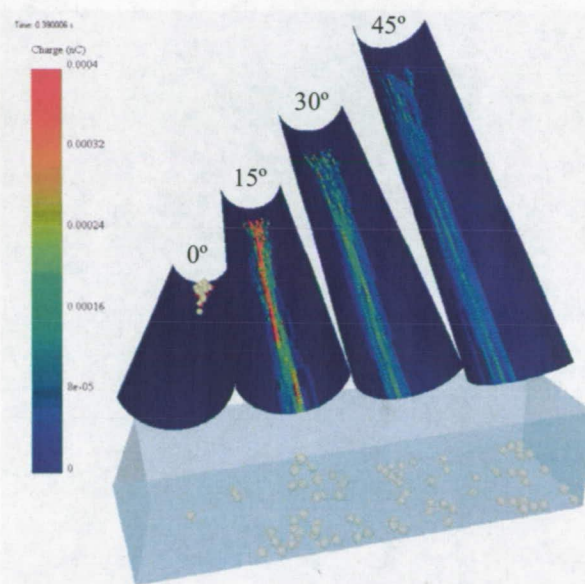


Figure 6. Charge build-up on the inclined surfaces at 0°, 15°, 30°, and 45°.

The zero degree slope generated the highest charge even though relatively little particle motion occurred [12]. Average charge on the spheres for each angle is shown in Fig. 7.

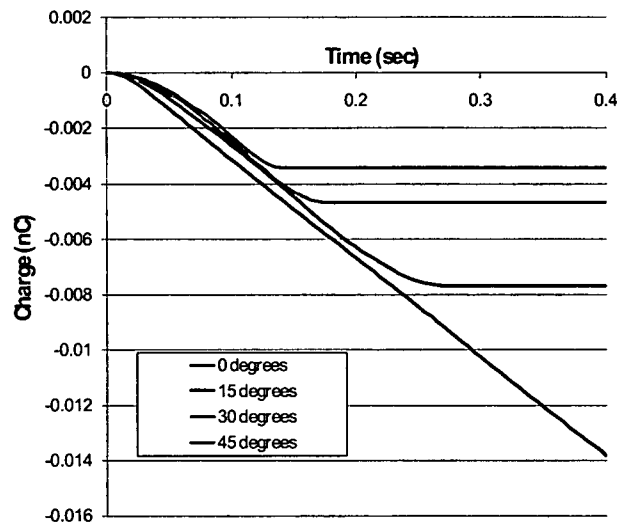


Figure 7. Average charge on the spheres for each angle [12].

The charge on the spheres at zero degrees in Fig. 7 is unphysical and is a consequence of contact time between the spheres and the inclined surfaces, not triboelectric charge exchange. This highlights a limitation of Greason's charge generation equation [3] in that it assumes rolling or sliding triboelectric contact between the two surfaces. The EDEM code will have to be revised to take non-motion contact into account.

V. FUTURE WORK

A. Additional Experiments

The experiments described in Section II need to be revised further to insure the removal or measurement of any initial charge on the spheres. This will include changing the experimental procedure to discharge the spheres as they are being loaded into the sphere cup by a deionizer and to load them slowly. Also, as mentioned in Section II B, the sphere cup can be replaced with a Faraday cup to measure the initial Q/m of the spheres prior to release and the resulting data compared to the previous experiments.

Additional materials will be used for the experiment to increase the data set. Additional sphere materials are: Copper, Carbon Steel, Acrylic, Polytetrafluoroethylene (PTFE), High Density Polyethylene (HDPE), Carbon, and Nylon 6/6. These spheres range in diameter from 1.6 mm to 2.34 mm.

The number of spheres will be reduced from previous experiments [1] from 500 to 250. This number will still allow flow patterns to be observed on the plane and facilitate the discharge of the spheres prior to the start of the experiment.

B. Addition of the Dielectrophoretic and Van der Waals Forces

KSC and Glenn Research Center (GRC) are engaged with DEM Solutions, Inc. to add advanced electrostatic and mechanical forces to the DEM software produced by DEM Solutions, Inc. KSC is assisting DEM Solutions, Inc. to add the dielectrophoretic force to the software. The dielectrophoretic force is the force exerted on the induced dipole moment of an uncharged dielectric particle by the presence of a non-uniform electric field [8]. This is the force that moves the dipolar Lunar and Martian regolith simulants off of KSC's dust screen [2]. The basic equation of the dielectrophoretic force is

$$\vec{F}_{DEP} = 2\pi\epsilon_1 R^3 \left(\frac{\epsilon_2 - \epsilon_1}{\epsilon_2 + 2\epsilon_1} \right) \vec{\nabla} E^2 \quad (10)$$

where ϵ_1 is the electric permittivity of the medium, ϵ_2 is the electric permittivity of the particle, R is the particle radius, and E is the non-uniform electric field [8]. Eq. (10) is valid for most non-uniform electric fields but if the non-uniformity of the field is very large (an approximate definition for "large" is where the non-uniform electric field is stronger than other fields or forces present), then a multipolar treatment is necessary [8][9]. The multi-polar force acting on a sphere with the electric field in the z-direction [8] is given by

$$F_z = \frac{2\pi\epsilon_1 K R^{2n+1}}{n!(n-1)!} \frac{\partial}{\partial z} \left(\frac{\partial^{n-1} E_z}{\partial z^{n-1}} \right)^2 \quad (11)$$

where $K = \frac{\epsilon_2 - \epsilon_1}{\epsilon_2 + 2\epsilon_1}$ (also called the Clausius-Mossotti factor).

When $n = 1$, Eq. (10) is recovered. The question to be answered is how intense of a field gradient is required for higher multipolar terms of Eq. (11) to become significant? Reference [9] indicates that higher multipoles of the dielectrophoretic force are not negligible within a few particle diameters unless the external field is weak.

Van der Waals forces is the term generally ascribed to intermolecular forces other than covalent or electrostatic [10][11]. In more macroscopic systems, sub-micron particles can adhere to each other or to surfaces via Van der Waals forces alone. GRC will provide the necessary theoretical support to DEM Solutions, to incorporate these forces into EDEM and provide experimental verification of the resulting simulation data.

VI. ACKNOWLEDGEMENTS

The authors would like to acknowledge NASA, Kennedy Space Center, Applied Technology Directorate and DEM Solutions, Inc. for their assistance in this work.

REFERENCES

- [1] M. D. Hogue, C. I. Calle, P. S. Weitzman, D. R. Curry, "Calculating the trajectories of triboelectrically charged particles using Discrete Element Modeling (DEM), *Journal of Electrostatics* **66** (2008) pp. 32-38.
- [2] Calle, C.I., J.G. Mantovani, C.R. Buhler, A. Chen, J.S. Clements, S. Trigwell, E.E. Arens, J.M. McFall, and M.L. Ritz, "Dust Mitigation Technologies for Lunar Exploration," International Conference on Exploration and Utilization of the Moon, Sorrento, Italy, October 22-26, 2007.
- [3] W. D. Greason, "Investigation of a test methodology for triboelectrification", *Jour. Electrostat.* **49**, Issue 3-4 (Aug, 2000) pp. 245-256.
- [4] M. D. Hogue, E. R. Mucciolo, C. I. Calle, C. R. Buhler, "Two-phase equilibrium model of insulator-insulator contact charging with electrostatic potential", *Jour. Electrostat.* **63** (2005) pp. 179-188.
- [5] M. D. Hogue, E. R. Mucciolo, C. I. Calle, "Triboelectric, corona, and induction charging of insulators as a function of pressure", *Jour. Electrostat.* **65** (2007) pp. 274-279.
- [6] J. A. Edminister, Schaum's Outline Series, *Electromagnetics*, McGraw-Hill, 1979, ch.2.
- [7] J. D. Jackson, *Classical Electrodynamics*, 3rd ed., Wiley, 1999, ch.1.
- [8] T. B. Jones, *Electromechanics of Particles*, Cambridge University Press, 1995, Ch. 2.
- [9] M. Washizu, T. B. Jones, "Dielectrophoretic Interaction of Two Spherical Particles Calculated by Equivalent Multipole-Moment Method", *IEEE Transactions on Industry Appl.* Vol. 32, No. 2, March/April 1996.
- [10] V. A. Parsegian, *Van der Waals Forces A Handbook for Biologists, Chemists, Engineers, and Physicists*, Cambridge University Press, 2006.
- [11] J. I. Israelachvili, *Intermolecular & Surface Forces*, 2nd ed., Academic Press, 1992, Ch. 6.
- [12] D. R. Curry, Technical Correspondence, DEM Solutions, Inc. April 8, 2008.